Journal of Basic and Environmental Sciences

ISSN
Online:2356-6388
Print:2536-9202

Research Paper Open Access

Synthesis and characterization of cerium oxide nanoparticles using combustion method

E. M. Qansowa, A. A. Ali, I. S. Ahmed

Chemistry Department, Faculty of science, Benha University, Benha, Egypt

Tel:+201211473447, E mail: esraaqansowa@gmail.com

Abstract

Cerium oxide nanoparticles were prepared by combustion method using citric acid as a fuel. The obtained cerium oxide nanoparticles characterized using XRD, FTIR, and DRS tools. The crystal size determined by XRD tool. The direct and indirect band gaps calculated by using the extracted data from DRS. The obtained cerium oxide nanoparticles are used as photocatalytic for degradation of amaranth (AM) and orange G (OG) dyes. The photodegradation efficiency of CeO_2 nanoparticles was 83% and 84% within 120 min for AM and OG, respectively.

Keywords: Cerium oxide nanoparticles, Combustion method, Band gap, photodegradation.

1. Introduction

Recently The attentions of researches. Has turned to study Ceira in the Phase of Nano and its Compounds because of Being the most abundant rare-earth metal (about 0.0046 wt.% of the Earth's crust), cerium is certainly an element of industrial relevance and its wide spread applications including antibacterial, antioxidant anticancer, The Therapeutic application drug- gene delivery system, antidiuretic property and tissue. Engineering, Nano ceira exhibits. Excellent antibacterial activity against

bacteria, applications as ultraviolet light absorbers, catalytic converters for automobile exhaust systems, solar cells, optics, oxygen sensors and other commercial and biomedical applications [1-3]. Cerium oxide exhibits a stable cubic fluorite (Fm3m space group) crystal structure with a lattice constant value of 5.4113 Å over a wide temperature range. Cerium oxide is a wide band gap semiconductor (Eg = 3.15–3.19 eV) at room temperature. It is particularly active in the UV range and has large exciton binding energy due to its unfilled 4f electronic configuration. The value of the bandgap energy depends on the preparation procedure and the presence of dopants and defects. The prevalence of oxygen defects increases as the nanoparticle size decreases, with their number being in direct relationship with the Ce3+ ion concentration [4-9]

Nano materials[10, 11] describe, in principle, chemical substances or materials of which a single unit is sized (in at least one dimension) between 1 and 100 nm. Nano materials research takes a materials science-based approach to nanotechnology, leveraging advances in Materials with structure at the Nano scale often have unique optical,electronic, thermo-physical or mechanical properties[12],[13]. Often the methods are divided into two main types, "bottom up" and "top down Synthesis of nanoceria can be carried out by various physical and chemical processes such as precipitation, hydrothermal, sol–gel, solvothermal, combustion and green synthesis. Different methods can produce Nano ceria with different forms, shapes, patterns, and sizes [14-16].

The use of reactive dyes has been increasing in various industries. Advanced oxidation technologies have gained importance to remove dyes from water. The leading one among these techniques is the degradation of dyes by a photochemical[17] process in in situ generating an oxidizing agent in water. Degradation of dyes with the photo catalytic[18] process has several advantages over other methods [19-21]. Combustion method[22] used due to its sutible characteristics and features; this approach can produce high unique of identical-sized nanoparticles on an industrial scale, so has more industrial use and is more widely used than alternative methods using the combustion process can be created High-purity, extremely homogenous oxides [23-26].

This paper describes how CeO2 nanoparticles was created using combustion method following by the calcination to increase crystallinity. XRD, FTIR, and DRS are some of the methods used to characterize the obtained cerium

oxide nanoparticles. The reflectance and optical properties of the synthesized Cerium oxide nanoparticles were investigated.

2. Experimental

2.1. Materials and reagents:

The chemicals utilized in this practical work were purchased and used as reached without any further purification. Cerium (III) nitrate hexahydrate $Ce(NO_3)_3 \cdot 6H_2O$, 99.9 %). Anhydrous Citric acid, (C6H8O7,) were purchased from Sigma-Aldrich Company, Hydrogen Peroxide (H_2O_2, 30%) 99%,amaranth dye ($C_{20}H_{11}N_2Na_3O_{10}S_3$) 98% ,Orange g dye ($C_{16}H_{10}N_2Na_2O_7S_2$) 98% distillated water.

Structure of dyes:

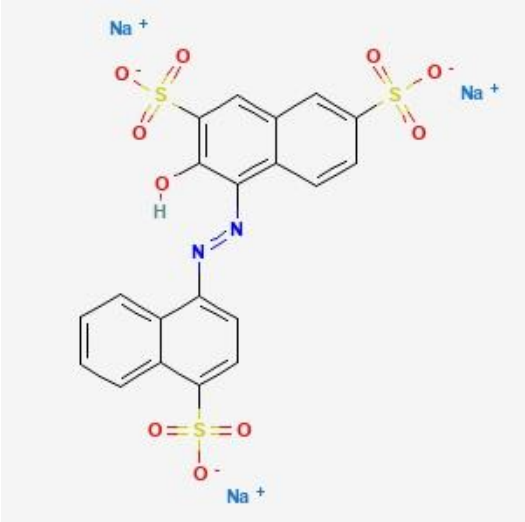

Amaranth dye

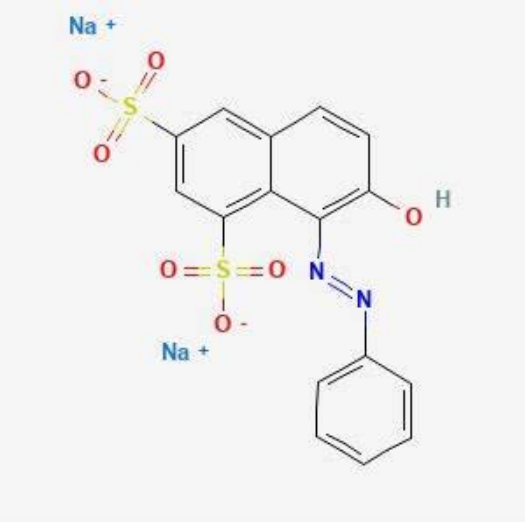

Orange g dye

2.2. Synthesis of cerium oxide nanoparticles via (combustion method):

0.01 mole of Cerium (III) nitrate hexahydrate were dissolved in 20 mL distilled water at room temperature, and calculated amount of citric acid as a fuel. The obtained solution was preheated at 120 °C on hotplate with magnetic stirring then added 0.01 mole from citric acid separately till forming homogenous solution, then, the solution ignited at 250 °C on hotplate, producing a white – pale yellow ash powder. The synthesized ash calcined at 500 °C for 30 min to obtain the pure crystalline cerium oxide nanoparticles. The cerium oxide nanoparticles synthesized from the combustion method, named as C1 after the calcination at 500/30 min.

2.3. Evolution of photocatalytic study:

50 mg of the fabricated cerium oxide (C1 sample) was added to 50 ml of each dye with initial concentration of 20 mg\L. Philips UV-mercury lambs (4*20 Wat at 365 nm) were used in the

photodegrading test as the irradiation source of UV-light. the obtained suspension was magnetically stirred for specific time. aliquots were the drawn at regular duration time and centrifuged to separate cerium oxide from dye solution. The filtrates of the dye's solution were analyzed by using a UV-Visible spectrophotometer. Photodegradation efficiency of dyes using the was estimated. A_0 and A are absorbance quantities of dye solution before and after degradation, respectively. Kinetic studies of the photodegradation of the testing dyes over the fabricated sample was tested using first-order models as represented in eq. (2) [27].

$$\boldsymbol{Degradation}\ \% = \left|\frac{(\mathbf{A_0} - \boldsymbol{A})}{\mathbf{A_0}}\right| \boldsymbol{x100} \quad (\mathbf{1})$$

$$\boldsymbol{Ln}\left(\frac{\boldsymbol{C_0}}{\boldsymbol{C_t}}\right) = \boldsymbol{Kt} \qquad (\mathbf{2})$$

2.4. Characterization:

The X-ray diffraction is employed to examine the structural and microstructural characteristics of created nanoparticles. The as-prepared samples were measured using FTIR spectrometer at room temperature from 4000 to 400 cm-1. Calcined sample's diffuse reflectance was investigated in ultraviolet-visible NIR range (200-2500 nm) using Jasco-V670 spectrophotometer and integrating sphere calibrated with barium sulfate as white standard.

3. Result and Discussion:

3.1. X-ray diffraction (XRD):

Figure (1) exhibits the XRD pattern of the synthesized cerium oxide nanoparticles (C1 sample) after calcination at 500°C for 30 min. According to XRD lines, crystalline structures appear due to the reference card No. 04-0593 at 2θ the peaks agree with the cerium oxide nanoparticles. The crystal size (D) of the cerium oxide nanoparticles (C1 sample) can be determined by using Scherrer formula (3).

$$\boldsymbol{D = 0.9\lambda/\beta cos\theta} \qquad (3)$$

Where, λ is the wavelength of X-ray (1.5406 A for Cu Kα), θ is the Bragg diffraction angle, and β is the x-ray full width half-maximum height (FWHM) of the XRD peak appearing at the diffraction angle θ. The obtained CeO2 average crystallite size (D) was found to be 10 nm.

3.2. FT-IR analysis:

The FT-IR spectra of the fabricated cerium oxide nanoparticle (C1 samples) is displayed in Figure (2). The peaks at 3,129 and 1,631 cm–1 are corresponding to the stretching and the bending vibrations of the adsorbed –OH groups, respectively.

The peak at 1,400 cm−1 can be assigned to the symmetric vibration of adsorbed C=O. The peaks at 1,111 and 616 cm–1 in the spectra assigned to the vibration modes of Ce–O–Ce and Ce–O, respectively inside CeO2 lattice. The weak absorption bands at 3,431 and 1,618.5 cm−1 are corresponding to the stretching and bending vibrations of hydroxyl groups respectively on the surface of CeO2 . The appeared peaks at 1,118 at 594 cm–1 in the spectra assigned to the vibration modes of Ce–O–Ce and Ce–O, respectively, inside CeO2 lattice [28, 29].

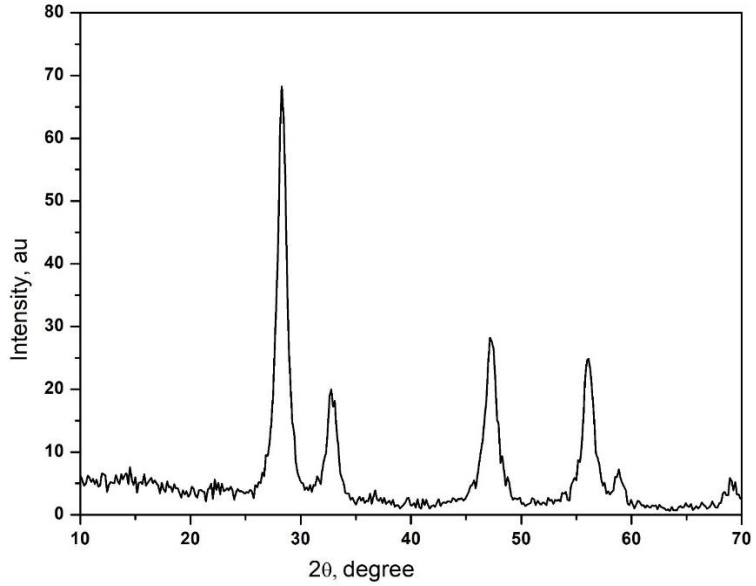

Fig (1): XRD pattern of the synthesized cerium oxide nanoparticles (C1).

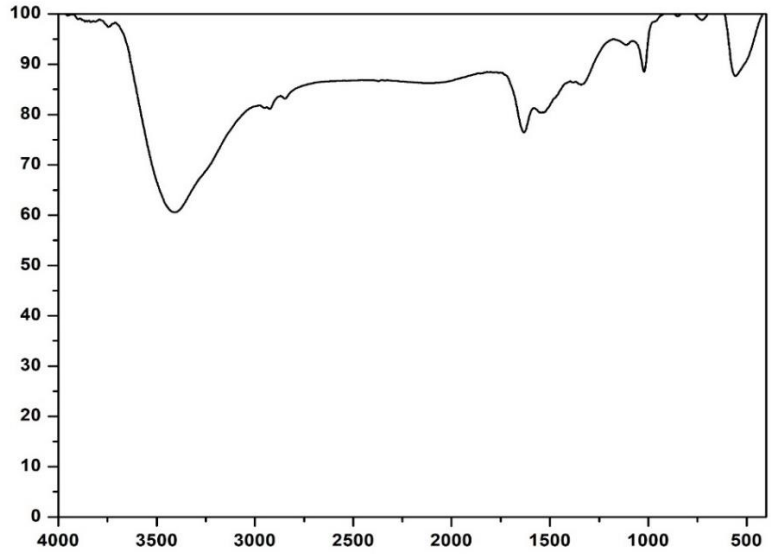

Fig (2): FTIR spectra of the synthesized cerium oxide nanoparticles after calcination (C1 sample).

3.3. Optical studies:

The calcined cirium oxide nanoparticles (C1 sample) are shown in Figure 3 was examined utilizing diffuse UV-VIS and NIR reflectance. Spectra displayed the measured reflectance between 200-2500 nm. The reflectance edge between 200-800 nm for C1 sample. The absorption coefficients (α) extracted from the experiment reflectance data using Kubelka Munk function as given by equation No (2).

$$\mathbf{F(R) = (K - M) = \alpha = \frac{(1 - R)^2}{2R}} \qquad (2)$$

Where, R is the experiment reflectance, F(R) is K-M function, α is absorption coefficients. the values of direct and indirect band gap are equal to 2.6 eV and 3 eV.

The UV-vis-NIR absorption spectra of cerium oxide nanoparticles (C1 sample) displayed in Figure 4. The broad absorption band between 200-500 nm as illustrated in Fig(4) .

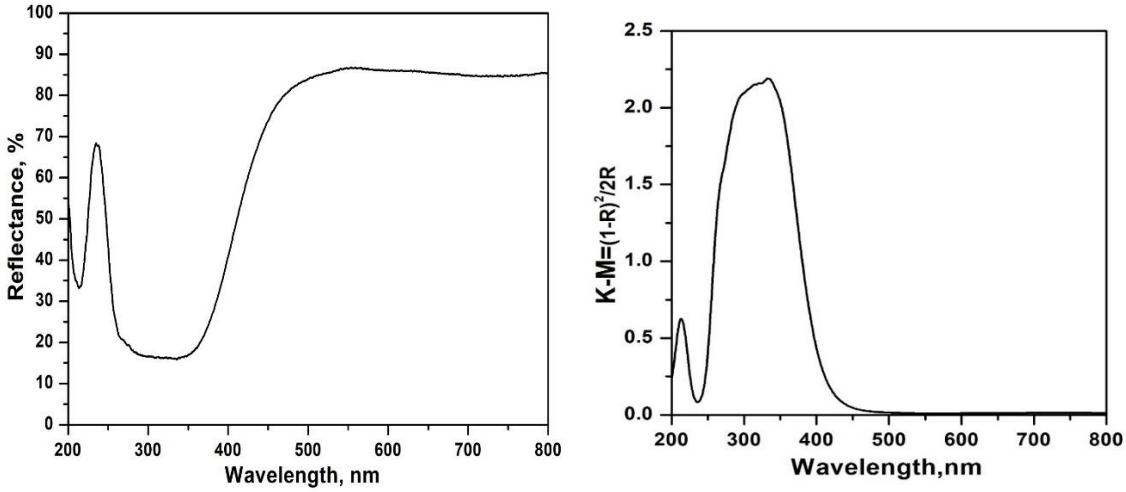

Fig (3): Reflectance and UV-VIS absorbance of the synthesized cerium oxide nanoparticles (C1 sample).

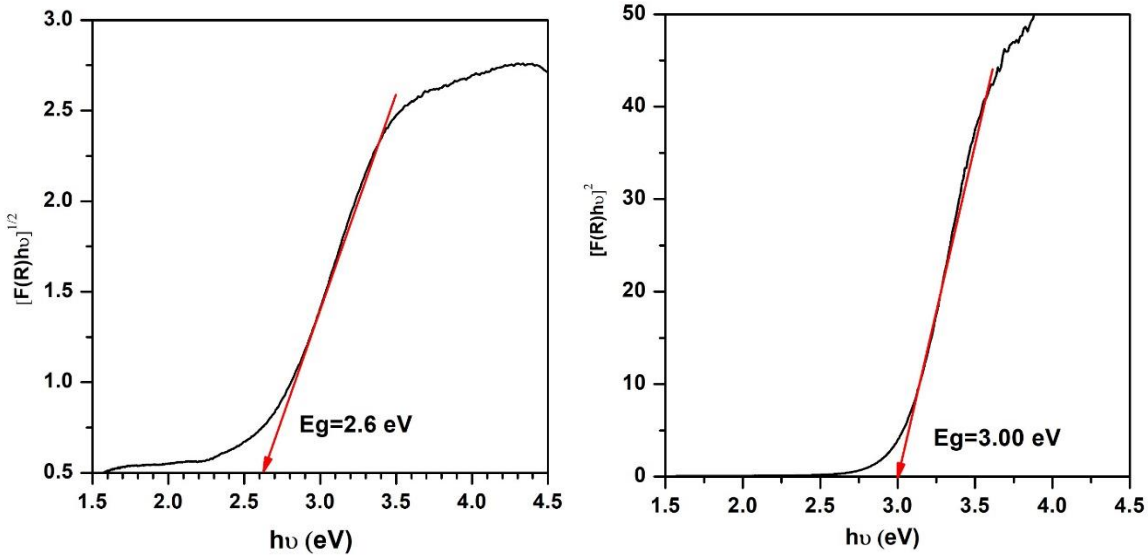

Fig (4): The direct and indirect band gap between of the synthesized of cerium oxide nanoparticles (C1 sample).

3.4. Photocatalytic studies:

Photocatalytic activities of synthesized cerium oxide have been studied by testing the degradation of AM and Orange G dyes under UV light. The intensity of the absorption bands of AM and OG dyes were recorded at (520) and (467) respectively. After one hour in dark the adsorption percentage of Amaranth dye ,Orange g dye over the C1 sample is 31%,29.7% respectively fig (5a)displays the spectra data of the degradation of AM and Orange G dyes under UV light was 69%and 32% respectively. , and fig (5b) displyes the spectra data of the degradation of AM and Orange G dyes under UV after addition of H2O2, the degradation was 83,6% and 84,6% respectively after time 120 min .fig(6) materialized the kinetic model in the form of the first order model of the degradation of amaranth and orange G dyes under UV light over the synthesized C1 sample .table 1outlined the degradation percentage,R2 values and rate constant (K,MIN-1) of AM ,and OG dyes respectively under UV light over the synthesized nps .

	SampelC1	
DYE	AM	OG
DY%	83.6%	84.6%
R^2	0.9961	0.9826
K,MIN^{-1}	0.0993	0.0421

Table (1): the degradation percentage,R^2 values and rate constant (K, MIN^{-1}) of AM ,and OG dyes respectively under UV light over the synthesized nps .

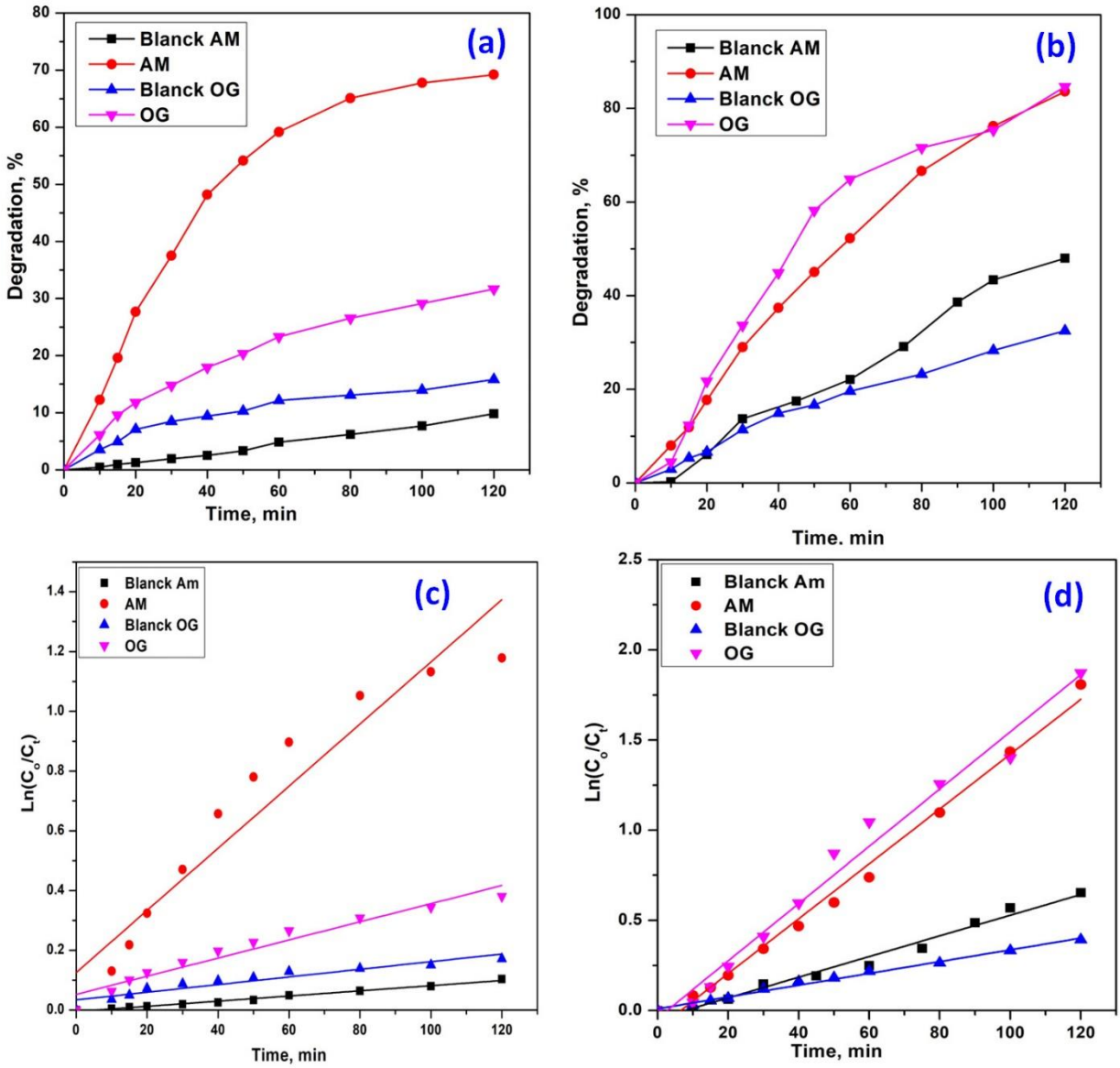

Fig (5): photodegradtion of AM. And OG dyes with H_2O_2 and without H_2O_2.

4. Conclusion:

Cerium oxide nanoparticles were synthesized using auto combustion method and the obtained ashes calcined at 500 °C for 30 min. various analytical methods, including Fourier transform infrared spectroscopy (FT-IR), and X-ray diffraction (XRD) are used for the characterization of the synthesized cerium oxide. The average crystallite size of the calcined cerium oxide was determined to be 10 nm. UV-VIS-NIR diffuse reflectance spectra of calcined cerium oxide displayed the reflectance edge between 200-500 nm. The degradation values of AM and OG dyes on the prepared cerium oxide recorder at 69%, 31% at120 min under the influence of UV irradiation respectively. The degradation values increased to be 83.6%, 84.6% with addition of the H_2O_2 respectively.

Acknowledgements

The authors express their thanks to Chemistry Department, Faculty of Science, Benha University, Egypt for support of the current research.

5. References:

[1] N. Thakur, P. Manna, J. Das, Synthesis and biomedical applications of nanoceria, a redox active nanoparticle, J Nanobiotechnology, 17 (2019) 84.

[2] T. Sahu, S. Singh Bisht, K. Ranjan Das, S.J.C.N. Kerkar, Nanoceria: synthesis and biomedical applications, Nanoscience, 9 (2013) 588-593.

[3] N. Fifere, A. Airinei, M. Asandulesa, A. Rotaru, E.L. Ursu, F. Doroftei, Investigating the Vibrational, Magnetic and Dielectric Properties, and Antioxidant Activity of Cerium Oxide Nanoparticles, 23 (2022) 13883.

[4] J. Calvache-Muñoz, F.A. Prado, J.E. Rodríguez-Páez, Cerium oxide nanoparticles: Synthesis, characterization and tentative mechanism of particle formation, Colloids Surf., A, 529 (2017) 146-159.

[5] R. Schmitt, A. Nenning, O. Kraynis, R. Korobko, A.I. Frenkel, I. Lubomirsky, S.M. Haile, J.L.J.C.S.R. Rupp, A review of defect structure and chemistry in ceria and its solid solutions, Chemical Society Reviews, 49 (2020) 554-592.

[6] B.R. Kumar, B. Hymavathi, T.S.J.J.o.S.A.M. Rao, Devices, Effect of the ceria dopant on the structural and dielectric properties of ZnO semiconductors, Advanced Materials, 3 (2018) 433-439.

[7] A. Ahmed, M.N. Siddique, T. Ali, P.J.A.S.S. Tripathi, Defect assisted improved room temperature ferromagnetism in Ce doped SnO2 nanoparticles, 483 (2019) 463-471.

[8] A.A.S. Ali, Sayed A Amin, Alaa S EL-Sayed, Sahar R, Synthesis and characterization of ZrO_2/CeO_2 nanocomposites for efficient removal of Acid Green 1 dye from aqueous solution, Mater. Sci. Eng., B, 269 (2021) 115167.

[9] A.A. Ali, S.R. El-Sayed, S.A. Shama, T.Y. Mohamed, A.S. Amin, Fabrication and characterization of cerium oxide nanoparticles for the removal of naphthol green B dye, Desalination and Water Treatment, 204 (2020) 124-135.

[10] I.S. Ahmed, H.A. Dessouki, A.A. Ali, Synthesis and characterization of new nano-particles as blue ceramic pigment, Spectrochimica Acta Part A: Molecular and Biomolecular Spectroscopy, 71 (2008) 616-620.

[11] Fabrication, structural and adsorption studies of zirconium oxide nanoparticles Benha Journal of Applied Sciences, 5 (2020) 245-253.

[12] M.A. Gabal, F. Al-Solami, Y.M. Al Angari, A. Awad, A.A. Al-Juaid, A. Saeed, Structural, magnetic, and electrical characterization of Sr-substituted LaFeO3 perovskite synthesized via sucrose auto-combustion route, Journal of Materials Science: Materials in Electronics, 31 (2020) 3146-3158.

[13] R. Sadri, M. Hosseini, S.N. Kazi, S. Bagheri, A.H. Abdelrazek, G. Ahmadi, N. Zubir, R. Ahmad, N.I.Z.J.J.o.c. Abidin, i. science, A facile, bio-based, novel approach for synthesis of

covalently functionalized graphene nanoplatelet nano-coolants toward improved thermo-physical and heat transfer properties, 509 (2018) 140-152.

[14] Y.W. Hartati, S.N. Topkaya, S. Gaffar, H.H. Bahti, A.E.J.R.a. Cetin, Synthesis and characterization of nanoceria for electrochemical sensing applications, 11 (2021) 16216-16235.

[15] M. Darroudi, M. Sarani, R.K. Oskuee, A.K. Zak, H.A. Hosseini, L.J.C.I. Gholami, Green synthesis and evaluation of metabolic activity of starch mediated nanoceria, Ceramics International, 40 (2014) 2041-2045.

[16] G. Sharmila, C. Muthukumaran, H. Saraswathi, E. Sangeetha, S. Soundarya, N.M. Kumar, Green synthesis, characterization and biological activities of nanoceria, Ceram. Int., 45 (2019) 12382-12386.

[17] M.Y. Nassar, A.A. Ali, A.S. Amin, A facile Pechini sol-gel synthesis of TiO2/Zn2TiO2/ZnO/C nanocomposite: an efficient catalyst for the photocatalytic degradation of Orange G textile dye (vol 7, pg 30411, 2017), RSC ADVANCES, 7 (2017) 33257-33257.

[18] M.A. Draz, H.H. El-Maghrabi, F.S. Soliman, H. Selim, A.A. Razik, A.E.-s. Amin, Y.M. Moustafa, A. Hamdy, A.A.J.J.o.N.R. Nada, Large scale hybrid magnetic ZnFe 2 O 4/TiO 2 nanocomposite with highly photocatalytic activity for water splitting, 23 (2021) 1-10.

[19] Q. Liu, Pollution and treatment of dye waste-water, in: IOP conference series: earth and environmental science, iop publishing, 2020, pp. 052001.

[20] D. Karadeniz, N. Kahya, F.B.J.J.o.P. Erim, P.A. Chemistry, Effective photocatalytic degradation of malachite green dye by Fe (III)-Cross-linked Alginate-Carboxymethyl cellulose composites, 428 (2022) 113867.

[21] Z. Kalaycıoğlu, B. Özuğur Uysal, Ö. Pekcan, F.B. Erim, Efficient Photocatalytic Degradation of Methylene Blue Dye from Aqueous Solution with Cerium Oxide Nanoparticles and Graphene Oxide-Doped Polyacrylamide, ACS Omega, 8 (2023) 13004-13015.

[22] M. Gabal, E. Al-Harthy, Y. Al Angari, A. Awad, A. Al-Juaid, A. Abdel-Daiem, A.J.J.o.S.-G.S. Saeed, Technology, Recovery of Mn 0.8 Zn 0.2 Fe 2 O 4 from Zn–C battery: Auto-combustion synthesizes, characterization, and electromagnetic properties, 100 (2021) 526-537.

[23] A.A. Ali, E.A. El Fadaly, N.M. Deraz, Auto-combustion fabrication, structural, morphological and photocatalytic activity of CuO/ZnO/MgO nanocomposites, Materials Chemistry and Physics, 270 (2021) 124762.

[24] C.E. Jeyanthi, R. Siddheswaran, P. Kumar, M.K. Chinnu, K. Rajarajan, R.J.M.C. Jayavel, Physics, Investigation on synthesis, structure, morphology, spectroscopic and electrochemical studies of praseodymium-doped ceria nanoparticles by combustion method, 151 (2015) 22-28.

[25] S. Patil, H.P.J.M.S.f.E.T. Dasari, Effect of fuel and solvent on soot oxidation activity of ceria

nanoparticles synthesized by solution combustion method, 2 (2019) 485-489.

[26] A.A. Ali, S.A. Shama, S.R. EL-Sayed, Fabrication, structural and adsorption studies of zirconium oxide nanoparticles, J Benha Journal of Applied Sciences, 5 (2020) 245-253.

[27] A.A. Ali, I.S. Ahmed, A.S. Amin, M.M. Gneidy, Auto-combustion Fabrication and Optical Properties of Zinc Oxide Nanoparticles for Degradation of Reactive Red 195 and Methyl Orange Dyes, J. Inorg. Organomet. Polym Mater., 31 (2021) 3780-3792.

[28] A.A. Ali, E.A. El Fadaly, N.M.J.M.C. Deraz, Physics, Auto-combustion fabrication, structural, morphological and photocatalytic activity of CuO/ZnO/MgO nanocomposites, 270 (2021) 124762.

[29] S.V. Gupta, M.J.I.J.o.E.A.C. Ahmaruzzaman, CeO2/Fe3O4/g-C3N4 nanohybrid for adsorptive removal of Rose Bengal from aqueous stream, 104 (2024) 1517-1536.